On the role of triethylene glycol in the preparation of highly active Ni-Mo/Al_2O_3 hydrodesulfurization catalysts: a spectroscopic study.

Aída Gutiérrez-Alejandre[a], Geovani Laurrabaquio-Rosas[a], Jorge Ramírez[a] and Guido Busca[b]

[a] UNICAT, Depto. de Ingeniería Química, Facultad de Química, Universidad Nacional Autónoma de México, Cd. Universitaria, México, DF 04510, Mexico

[b] Laboratorio di Chimica delle Superfici e Catalisi, Dipartimento di Ingegneria Civile, Chimica e Ambientale, Università di Genova, Fiera del Mare, pad. D, I-16129 Genova, Italy.

Abstract.

The interaction of triethylene glycol (TEG) with alumina and its role in preparing improved NiMo/Al_2O_3 hydrodesulphurization catalysts was investigated by spectroscopic methods. The FT-IR study shows that TEG adsorbs mainly on the corners and edges of alumina microcrystals where the strongest Lewis sites and the higher νOH frequency hydroxyl groups are mainly located. It is also observed that the Mo=O stretching vibration of surface molybdenyl groups in the oxide catalyst precursor is shifted down in the presence of TEG, indicating a lower interaction with the surface. The IR spectra of CO adsorbed on the reduced/sulfided NiMo catalysts confirm that the amount of promoted phase increases in the samples prepared with TEG. Accordingly, the activity measurements in the HDS of 4,6-dimethyldibenzothiophene show that the catalyst prepared with TEG is more active than the one prepared without it. It is proposed that TEG and its decomposition products, formed upon heating (mainly acetates) occupy preferably the strongly interacting edge and corner sites of the alumina crystals, forcing the Mo and Ni species to migrate mainly to the plane faces. This weakens the metal-support interaction allowing a better sulfidation and, at the same time, favors the Ni-Mo interaction and the formation of the promoted NiMoS phase.

Keywords: triethylene glycol, hydrodesulfurization, infrared spectroscopy

1. Introduction

The strict regulations in the content of contaminants, especially sulfur, in transport fuels has induced a strong improvement in the quality of air, which is expected to continue for the near future. In particular, improvements on the activity of hydrodesulphurization (HDS) catalysts and the strengthening of the operating conditions (P and T) of the HDS processes allowed a strong reduction in the sulfur content in fuels. In the European Union the limit on automotive fuels (for both gasoline and Diesel fuel) is 10 ppm.

Improved HDS catalysts based on Co- or Ni-promoted MoS_2 or WS_2-supported on alumina have been obtained, at least in part, thanks to the reformulation of the preparation procedure allowing to obtain better dispersion and higher levels of promotion during the catalyst preparation. One of the methods to enhance the activity of HDS catalysts is through the use of organic additives. Among others, some patents cite tri-ethylene glycol (TEG) as a useful additive in this respect [1-3].

Several studies have been published in the current literature concerning the effects of ethylene glycols to HDS catalysts but most of them concern the preparation of Co-Mo/Al_2O_3 catalysts [4-9]. As discussed by Costa et al. [9] different opinions are reported for the effect of TEG on the performance of Co-Mo/Al_2O_3 HDS catalysts. In particular, conflicting data are reported concerning the effect of the organic additive on the sulfidation behavior, while it seems well established that the additive hinders the interaction between the active phase precursors and alumina and that enhances the dispersion of the Co and Mo species. As a consequence, more cobalt atoms are available to promote the MoS_2 crystallites formed upon sulfidation. In contrast, the preparation of Ni-Mo/Al_2O_3 catalysts with ethylene glycol has been the object of less attention. Escobar et al. [10] studied the effect of ethylene glycol (EG) on the preparation Ni-Mo-P/Al_2O_3 catalysts. From TPR experiments it was found that addition of ethylene glycol to the impregnating Ni-Mo solution resulted in a decreased interaction between the alumina support and the Ni and Mo phases. Dispersion and sulfidability showed opposite behavior with EG addition; sulfidability decreased while dispersion of the Mo phases increased. Yin et al. [11] made a study on the impregnating solution and found that by adding glycol, the presence of the $H_x[P2Mo_5O_{23}]^{(6-x)-}$ heteropolycompound is favored over several other species. No references were found for studies with NiMo catalysts using triethylene glycol as organic additive.

In the present paper we will perform a detailed IR spectroscopic study of Ni-Mo/Al_2O_3 catalysts prepared with and without TEG to understand the interaction of the additive with the support and active phases, and the changes induced by the organic additive on the structure and sulfidation of the Mo and Ni surface species, that lead to an increased HDS activity.

2. Experimental

2.1 Solutions and catalysts preparation.

Solutions containing water, TEG, nickel nitrate $Ni(NO_3)_2 \cdot 6\ H_2O$ and ammonium heptamolybdate $(NH_4)_6Mo_7O_{24}\ 4H_2O$, were prepared by contacting appropriated amounts of the different components and ageing under stirring for 2 h.

Commercial γ-Al_2O_3 from Sasol with BET surface area of 212 m^2/g was used as support. The γ-Al_2O_3-TEG sample was prepared by impregnation of alumina with an aqueous solution of triethylene glycol. The solid powder was dispersed in the solution at room temperature for 2 h, and then the slurry was dried in an oven at 373 K during 24 h.

The NiMoT/γ-Al_2O_3 catalyst, denoted as NiMoT, was prepared by incipient wetness successive impregnation; in the first step the alumina support was impregnated with an aqueous solution of ammonium heptamolybdate with the appropriate molybdenum concentration to get 2.8 Mo atoms/nm^2. After 2 h, the solid was dried at 373 K during 24 h. Later, the resulting powder was impregnated with a water solution of nickel nitrate and triethylene glycol mantaining a Ni/(Ni+Mo) atomic ratio of 0.33 and a TEG/Ni molar ratio = 1.2 respectively. Finally, the impregnated sample was dried at 373 K during 24 h.

The conventional NiMo catalyst, without citric acid, used as reference; was prepared using the same procedure as for NiMoT but in this case, after the drying step; the solid was calcined at 673 K for 4 h.

2.2 Spectroscopic characterization

IR spectra were collected (100 scans, 4 cm^{-1} resolution) using a Nicolet Nexus FT-IR instrument. Pure powder pressed disks of the catalyst were activated by outgassing at several temperatures, from room temperature up to 773 K using an infrared cell connected to a conventional gas manipulation/outgassing vacuum line.

Pyridine adsorption. The adsorption of pyridine was performed by contacting the samples (wafer of ~ 10 mg/cm^2), preactivated by outgassing at 573 K, with 1 Torr of pyridine vapour evaporated under vacuum. After that the IR spectrum was collected.

CO adsorption on sulfided samples. For CO adsorption experiments, self-supporting wafers of ~7.5 mg/cm^2 of pure catalyst powder were made, placed in the IR cell, and then sulfided at the same conditions as used in the catalytic activity tests (673 K for 4 h in H_2S/H_2 mixture (15% v/v)). Subsequently, the cell was outgassed in vacuum at 723 K for 2 h. Then, CO adsorption at 100 K was performed by adding small pulses of CO up to a pressure of 1 Torr equilibrium. The spectra were taken with a Thermo Nicolet 6700 FTIR spectrophotometer with a resolution of 4 cm^{-1} and 100 scans per spectrum. For the quantitative analysis the integrated molar extinction coefficients of CO adsorbed on the sulfided catalysts were determined in the IR cell at liquid nitrogen temperature (100 K) by introducing several small doses of CO (0.005 Torr).

High Resolution Electron Microscopy. HRTEM micrographs of the sulfided catalysts were obtained with a JEOL 2010 transmission electron microscope operating at 200 kV with 1.9 Å point to point resolution. Prior to the analysis, the samples were sulfided at the same conditions as for the catalytic activity tests. The sulfided samples were dispersed by ultrasonication in heptane for 20 min, and a drop of the supernatant liquid was placed on a holey carbon film supported on a copper grid. For the statistical analysis of the size and stacking distribution of MoS_2 crystallites, more than 300 crystallites were measured. From these measurements a value for MoS_2 dispersion was obtained from the calculation of Mo_{edge}/Mo_{total}, assuming hexagonal MoS_2 crystallites.

UV-Vis-DRS. Diffuse reflectance spectra were carried out in the UV–Visible range using a JascoV-570 spectrometer (Perkin Elmer) equipped with an integration sphere.

2.3 Catalytic activity test

Prior to the catalytic activity test, the catalysts precursors were activated using 40 mL/min of H_2S/H_2 mixture (15% v/v) at 673 K for 4 h. The catalytic activity tests were perfomed in a Batch Parr reactor at 593 K and 1200 psig of hydrogen. The reaction mixture was composed by n-decane and 4,6-Dimethyldibenzothiophene (1000 ppm as S). The analysis of reaction products were performed using an HP 6890 gas chromatograph, equipped with a flame ionization detector. The products were analyzed each 30 min during the first three hours and then each hour.

3. Results and discussion

3.1. Catalytic activity.

The catalytic activity performances obtained for NiMoT and NiMo catalysts are summarized in Table 1. The data clearly show that NiMoT, prepared using TEG as organic additive, is about 2.5 times more active than the catalyst prepared without TEG. It is also observed that the transformation through the direct desulfurization route (DDS) increased 1.4 times while that through the HYD route increased 2.8 times. Thus the HYD/DDS ratio increased 1.9 times. Since the DDS takes place in coordinatively unsaturated sites on the edges of the NiMoS phase, the increase in the DDS indicates an increase in the active phase dispersion. On the other hand, the increase in the transformation through the HYD route, that takes place mostly in the BRIM sites [12], signals a better sulfidation of the active phase.

The significant increase in HDS activity obtained using TEG (2.5 times) cannot be fully explained by an increase in dispersion of only 13 % obtained from the HRTEM observations of the catalyst samples. Therefore, to explain the observed changes in activity, an IR study of the interactions of TEG with the alumina support and with the catalyst (before sulfidation) was undertaken.

3.2 IR study of the interaction of TEG with alumina.

In Figure 1 the infrared spectra of alumina with TEG, γ-Al_2O_3-TEG, recorded after outgassing at increasing temperature up to 773 K, are reported. The spectrum of pure γ-Al_2O_3 outgassed at 773 K is also reported for comparison. In this figure, the adsorbed TEG species are responsible for the presence of several bands in the γ-Al_2O_3-TEG IR spectra, which are not present in the spectrum of pure γ-Al_2O_3. These bands are shown in the form of subtraction spectra (where the spectrum of pure alumina is subtracted), in Figure 2, where the IR bands can be compared with those of pure liquid TEG deposed on a KBr disk. The strong bands in the 3000-2700 cm^{-1} region are associated to C-H stretching vibrations, ν_{CH}. In the region below 1500 cm^{-1}, the bands observed at 1454, 1350, 1299, 1251, 1113 and 1079 cm^{-1} are attributed essentially to adsorbed TEG species formed by

δCH_2, δCOH, γCH_2, τCH_2 and two different νCO vibrations respectively [13]. The band at 1647 cm^{-1} in the spectrum of liquid TEG can be assigned to water impurities (δH_2O). The shoulder at 1630 cm^{-1} in the γ-Al_2O_3-TEG spectrum can be assigned to adsorbed water arising from these water impurities in TEG.

The spectrum of γ-Al_2O_3-TEG shows, after outgassing at room temperature, a peak at 1598 cm^{-1} which is not evident in the spectrum of TEG. This peak is associated to small amounts of carboxylate impurities which are present in the spectrum of γ-Al_2O_3, likely due to the presence of residual organic impurities from the preparation method of Sasol aluminas (Ziegler process from aluminum alkoxides [14]).

In the OH stretching region the spectrum of γ-Al_2O_3-TEG shows, after outgassing at room temperature, a broad absorption centered near 3630 cm^{-1} tailed towards lower frequencies. During progressive heating treatment upon outgassing, it is evident that the spectrum of γ-Al_2O_3-TEG gradually modifies. The progressive disappearance in the range 373-573 K of the broad shoulder near 1630 cm^{-1} (Figure 1) is observed upon outgassing under heating. Correspondingly, a change in the shape of the absorption in the OH stretching region occurs. In fact the main maximum near 3630 cm^{-1} disappears, while two components at ~3670 cm^{-1} (sharp, weak) and at ~3550 cm^{-1} become evident. This indicates that adsorbed water, responsible for the bands centered at 3630 and 1630 cm^{-1} (νOH's and δH_2O, respectively) desorbs while hydroxyl groups are still at the surface. Additionally, dehydroxylation of the alumina as well as dissociation of the TEG's hydroxyl groups may also occur, in agreement with a change in the shape of the absorption in the 1200-1000 cm^{-1} range, due to C-O(H)

The spectrum of γ-Al_2O_3-TEG in the 3800-3500 cm^{-1} region (OH-stretchings) after outgassing at 773 K is significantly different from that of pure alumina activated in the same conditions. The spectrum of pure γ-Al_2O_3, after heating at 773 K, shows the bands of surface free (non H-bonded) hydroxyl groups at 3733 and 3692 cm^{-1}, with possibly some additional weak component at higher frequency. A broad band at 3565-3500 cm^{-1} is also evident, due to H-bonded hydroxyl groups. After outgassing at 773 K only very weak bands of free hydroxyls are observed in the spectrum of γ-Al_2O_3-TEG. The subtractions reported in the right side of Figure 2 confirm this, showing that the spectra of γ-Al_2O_3-TEG have higher absorption than the pure γ-Al_2O_3 one in the region below 3650 cm^{-1}, thus showing more H-bonded OHs. In contrast, the spectrum of γ-Al_2O_3-TEG is weaker than that of γ-Al_2O_3 at higher frequencies in the region of free OHs (negative bands in the subtraction spectrum). This shows that TEG species on γ-Al_2O_3-TEG perturb or substitute free hydroxyl groups of alumina, while producing more H-bonded hydroxyl groups, either of the Al-OH or of the C-OH type.

These data show that adsorption of TEG indeed involves an interaction with the surface hydroxyl groups of alumina.

After heating, starting from 473 K, the bands due to TEG species adsorbed on γ-Al_2O_3-TEG clearly change. The absorption due to CH stretching changes in shape, decreasing the lower frequency component with respect to the higher frequency one that almost disappears, leaving only a weak feature centered near 2900 cm^{-1} at 773 K. In the lower frequency region the spectrum progressively modifies. The shape of the strong CO stretching bands in the region, quite different from the corresponding bands in pure TEG, and is modified by outgassing at 300-573 K. All the bands in the 1400-1000 cm^{-1} region progressively fully disappear at 773 K while two main bands become evident at 1573 and 1477 cm^{-1}, possibly with a component near 1400 cm^{-1}. The resulting spectrum after outgassing at 773 K corresponds to that of carboxylate species (COO asymmetric and symmetric stretching, respectively) very likely acetate species adsorbed on alumina [15] coming from TEG decomposition.

The IR spectra thus show that TEG is stable on the surface, although likely partially converted to dissociated species, at least until 573 K, while it decomposes to acetate species above this temperature. Acetate species are still observed at 773 K. Both TEG and acetate species interact with or even displace most of the free surface hydroxyl groups.

To reveal the modifications of the surface properties of γ-Al_2O_3 by adsorbed TEG, the IR spectra of pyridine adsorbed on both γ-Al_2O_3 and γ-Al_2O_3-TEG, previously outgassed at 473 K, have also been investigated (Figure 3).

As it is well known [16], the spectrum of pyridine presents, in the 1800-1400 cm^{-1} region, four strong bands (ring vibrations) denoted as 8a, 8b, 19a and 19b modes, centered, in the liquid, at 1583, 1577, 1481 and 1436 cm^{-1}. The 8a and 19b modes are both sensitive to interaction with Lewis sites, being shifted up with the strength of the Lewis site.

The spectra of pyridine adsorbed on γ-Al_2O_3 and γ-Al_2O_3-TEG have a remarkably different intensity, showing that the adsorbed amount of pyridine is significantly decreased (nearly 39 % less) by the presence of TEG. Three definite bands are observed in the 8a/8b region at ca 1612, 1593 and 1580 cm^{-1} assigned to two 8a modes (at least two different adsorbed species) and the 8b mode of adsorbed pyridine. An additional shoulder is evident at higher frequencies (ca 1622 cm^{-1}).

Also bands at 1482 (weak) and 1441 cm^{-1}, due to 19a and 19b modes of adsorbed pyridine are observed before outgassing. The spectra of both samples show the presence of four different pyridine species. The bands at ca 1580 and 1440 cm^{-1} can be predominantly due to 8a and 19b modes of a weakly bonded, likely H-bonded, species, which disappears by outgassing at room temperature. After outgassing at r.t. three different pyridine species leave, characterized by three well resolved 8a bands at 1593, 1612 and 1621 cm^{-1}, the last being evident as a shoulder. The band at 1577 cm^{-1} is due to the non-sensitive 8b mode of all three species, unsplit. The bands associated to the 8a mode shift slightly to higher frequency while decreasing in intensity upon outgassing at increasing temperature. The presence of at least three different Lewis sites on

aluminas has already been reported by many authors [14]. As expected, none of the solids present significant Brønsted acidity bands attributed to pyridinium ion.

The bands of pyridine adsorbed on Lewis sites on the two surfaces, before and after contacting with TEG, are located nearly at the same frequencies, but the intensity of the bands associated to pyridine adsorbed on the strongest sites (8a band at 1614 cm^{-1} and shoulder at 1622 $cm^{-1,}$ corresponding to 19b bands at 1460-1450 cm^{-1}) are clearly reduced (by nearly 70 %) on γ-Al_2O_3-TEG with respect to γ-Al_2O_3 than those due to physisorbed species and species bonded to weaker Lewis sites.

A thorough analysis of the available data [16] led us to conclude that pyridine, responsible for 8a modes at 1614 and 1622 cm^{-1}, is interacting via a Lewis-type interaction with Al^{3+} in coordination three (four including pyridine), likely located on the edges, corners, or similar defects on the alumina crystal surface. A similar conclusion was obtained for OH's absorbing at higher frequencies that are expected to be bonded to tetracoordinated Al ions mainly on edges and corners [16]. The IR study of adsorption of TEG (Figures 1 to 3) thus suggests that TEG primarily interacts with the more exposed and strongest sites (Lewis sites and hydroxyl groups) of alumina, located in edges and corners, leaving less exposed sites located on plane faces largely free.

The interaction of TEG with the alumina surface is evidently strong, since adsorbed TEG decomposed only after heating above 573 K, before being desorbed. The interaction is also stronger than that of water, which is in fact desorbed in the 300-573 K range, when TEG is still stable on the surface. In any case, the decomposition of adsorbed TEG at 773 K leaves on the surface carboxylate species, likely mainly acetates, still interacting with corner and edge sites. Thus, taking into account the temperature used for sulfidation and reaction on the sulfided catalysts, the use of TEG could "irreversibly" poison the strongest sites of alumina located on edges and corners.

3.3 IR study of the NiMoT catalyst precursor.

In Figure 4, the IR spectra of the NiMoT catalyst precursor after outgassing at different temperatures are reported. In the right section the 1200-800 cm^{-1} region of the spectra obtained after outgassing at 573 to 773 K are expanded. In Figure 5 the subtraction spectra are reported in the 1700-900 cm^{-1} region. They are obtained by subtracting from each spectrum that of NiMoT after outgassing at 773 K.

The first spectra in both figures refer to NiMoT dried at 373 K. The spectra show clearly the absorption at 1113 and 1047 cm^{-1}, due to CO stretchings of adsorbed TEG. After outgassing the position of this band shifts a little bit the main maximum being at 1070 cm^{-1}, as above for the γ-Al_2O_3-TEG sample (see Figure 5). Similarly, the CH stretching modes of adsorbed TEG are evident at 2946 and 2884 cm^{-1}. The strong broad absorption in the region 3500-2700 cm^{-1} and the sharper one at 1448 cm^{-1} are due to ammonium ions (νNH's and $\delta_{as}NH_4$ respectively). In fact these

features disappear in parallel by outgassing in the range 300-573 K, due to the decomposition of ammonium ions with evolution of gas phase ammonia. Traces of adsorbed ammonia are associated to the weak band at 1608 cm^{-1} ($\delta_{as}NH_3$). The very strong band at 1313 cm^{-1} is very likely associated to the component observed in the range 1500-1530 cm^{-1} corresponding to bicoordinated nitrate species. Also these features fully disappeared upon outgassing at 573 K. The spectra of the NiMoT sample look very similar to those of γ-Al_2O_3-TEG in the region above 1050 cm^{-1}, after outgassing at 573-773 K.

The similarity of the spectra of TEG in the NiMoT and in the γ-Al_2O_3-TEG samples may indicate that not significant chelation of Ni ions by TEG occurs and that the primary interaction of TEG is with alumina. The spectra of the NiMoT catalyst show, in the region near 1000 cm^{-1}, a sharp absorption, which is not present on the alumina sample. This absorption, evident as an edge in Figure 4 because of the near cut-off limit due to the absorption due to bulk Al-O vibrations, clearly shifts from near 985 cm-^{1} to near 1025 cm^{-1} when samples is heated under vacuum above 473 K. Correspondingly, the subtractions reported in Figure 5 show a negative peak situated neat 1021 cm^{-1} in all spectra. The position of this band is typical of the Mo=O stretching of surface molybdenyl species [17,18] on alumina.

This behavior suggests that the presence of TEG causes a modification of the coordination state of molybdenum on alumina, with a lowering of the Mo=O molybdenyl bond order. According to the literature [18], the higher the Mo=O frequency, the lower the basicity of the other ligands around molybdenum. Thus, the data we report here suggest that either TEG interacts directly with molybdenyl ions, providing O-terminated ligands with lower basicity than alumina's oxide anions, or TEG shifts molybdenyl ions to less acido-basic sites. The overall results suggest that in the absence of TEG MoO^{4+} ions will largely adsorb on the more acido-basic sites located on edges and corners of the alumina crystals, being characterized, in these conditions by the Mo=O stretching near 1025 cm^{-1}. Only when in excess they will also depose on the plane faces, where it can take the coordination characterized by Mo=O stretching at 985 cm^{-1}. In the presence of TEG, instead, MoO^{4+} ions will be forced to shift predominantly over plane faces, being the edge sites "poisoned" by TEG. The partial decomposition of TEG to acetates starting to occur (incompletely) above 473 K will progressively free part of the edge sites, where MoO^{4+} ions can diffuse back.

3.4 UV-vis-NIR DR study of the catalyst precursors.

The UV-vis spectrum of the NiMoT catalyst precursor and of the conventionally prepared NiMo catalyst precursor both recorded in air without any pretreatments, are compared in Figure 6. They are also compared with the spectrum of a conventionally prepared 5 % NiO/Al_2O_3 catalyst and 8 % MoO_3/Al_2O_3 in their oxide form, as well as with the spectrum of bulk nanometric NiO.

In all cases, the strong absorption region observed above 28500 cm^{-1} is associated to charge transfer transitions (CTT) of the O^{2-} (2p) $\rightarrow$ Mo^{5+} (3d) and/or O^{2-} (2p) $\rightarrow$ Ni^{2+} (3d) that become, essentially, valence –to- conduction band transitions for finite bulk systems.

The spectra of MoO_3/Al_2O_3 at low loading have been reported by several authors [19-21]. The strong CTT band is centered, as usual, at about 44000 cm^{-1} (λ = 230 nm) in the case of hydrated "monomeric" molybdenyl species. The absorption decreases by increasing wavelength continuously down to be negligible just at the limit of the visible region, near 25000 cm^{-1}.

The spectrum of the conventionally prepared NiMo sample presents the strong absorption maximum at ca 41000 cm^{-1} possibly with a second maximum at ca 46300 cm^{-1} (216 and 244 nm), while the spectrum of NiMoT shows its main maximum at 41800 cm^{-1} (240 nm), possibly with a second component, not clearly defined because of the noise present near the limit of 200 nm of the UV source of the instrument.

As for comparison, we may remark that for highly dispersed Ni^{2+} on alumina the absorption here grows towards higher energies, the maximum being above 45000 cm^{-1} (below 220 nm). As discussed previously, by increasing the amount of Ni^{2+} on alumina first a strong absorption appears at 37000 cm^{-1}, assigned to very small NiO particles, then the spectrum of bulk NiO appears, with an almost continuous absorption with two maxima at 30000 and 41500 cm^{-1}, at very high Ni loadings. It seems quite reasonable to attribute the main maxima observed in the region 46000-40000 cm^{-1} predominantly to the O^{2-} (2p) $\rightarrow$ Mo^{5+} (3d) CT transition. The presence of Ni^{2+} induces a broadening of the low energy tail of the CT absorption, shifting towards the visible region, influenced by the O^{2-} (2p) $\rightarrow$ Ni^{2+} (3d) CT transitions where, however, other d-d components of Ni^{2+} also exist.

In the lower wavenumbers region, below 28500 cm^{-1}, the d-d transitions of Ni^{2+} are expected. It is clear that the spectra of the NiMo catalysts, which are very similar toeach other here, are very different from those of dispersed NiO/Al_2O_3 and NiO samples, suggesting that indeed a main electronic interaction of Ni occurs with Mo oxide species, predominant with respect to the interaction with alumina. The close similarity of the spectra of the two catalyst precursors in the Ni^{2+} d-d transitions suggests that the TEG additive does not perturbs the Ni species significantly.

The difference between the spectra of the NiMoT sample and that of the conventionally prepared NiMo catalyst seems to be mostly in the shape of the strongest band, in the UV region with the threshold limit shifting to the visible region and the main maximum shifting slightly in the reverse sense. It seems likely that the presence of TEG increases the perturbation of Mo species, with a slight shift of the maximum and a broadening of the lower wavenumber tail of the O^{2-} (2p) $\rightarrow$ Mo^{5+} (3d) CT transition.

According to the IR data discussed above, where it has been shown that the presence of TEG at the surface implies a lower frequency for surface Mo=O stretching modes, we can conclude that TEG influences the state of molybdenum, forcing it in a slightly different position or coordination

state where the interaction with nickel is increased. This would support that Mo ions are shifted at least in part from corners to plane faces by TEG.

3.5 IR spectra of adsorbed CO on sulfided NiMo catalysts.

In Figure 7 the IR spectra of CO adsorbed at low temperature on the sulfided conventionally prepared and TEG-containing NiMo catalysts are reported. The spectrum of the conventionally prepared NiMo catalyst agrees with that reported in the literature [22]. The main band at 2125 cm^{-1} is attributed to CO interacting with Ni^{2+} on the Ni-promoted MoS_2 phase, while the shoulder near 2060 cm^{-1} is attributed to CO adsorbing on Mo sites located near Ni ions in the same active phase. The absorption centered at 2106 and 2087 cm^{-1} should instead be associated to CO on non-promoted MoS_2 sites. The still strong band at 2220 cm^{-1} which has a shoulder at 2212 cm^{-1}, is associated to highly acidic Al^{3+} located in the edges and corners of the crystals. We can note that the spectrum is overall weak, much weaker than that found on pure alumina in these conditions. Additionally we can remind that unreduced/unsulfided Mo species does not adsorb CO being thus silent in this technique.

The spectrum of NiMoT is similar but shows stronger bands due to CO interacting with the NiMo sulfided species. A definite difference is observed in the region 2220-2170 cm^{-1}, where the band at 2200-2212 cm^{-1} is no more evident while a band at 2188 cm^{-1} is observed. This result confirms that TEG or its residuals such as acetate ions specifically interact with the strongest Al^{3+} ions, likely lowering their acidity. The definite change in the ratio between the band due to CO on NiMo sulfided species and that of CO on Al^{3+} on corners and edges would confirm that TEG favors a more extended formation of the active promoted NiMo sulfide species by shifting Mo from edges to plane faces.

The results from the catalytic activity data show that the NiMoT catalyst, i.e. the sulfided $NiMo/Al_2O_3$ catalyst prepared by two step impregnation, the second in the presence of TEG, is more active than a $NiMo/Al_2O_3$ prepared conventionally. The IR data suggest that TEG is adsorbed strongly on alumina, where it starts to decompose, in dynamic vacuum, only above 573-673 K, leaving on the surface even more stable acetate species. IR data also show that the presence of TEG influences the state of molybdenyl species, whose Mo=O stretching frequency is observed at lower frequency (985 cm^{-1}) than when TEG is absent (1025 cm^{-1}), or start to be partly decomposed. Additionally, the UV-vis data indicate that the presence of TEG does not modify significantly the d-d transitions of Ni^{2+}, while shifting and broadening the charge transfer transition region, where the O^{2-} (2p) $\rightarrow$ Mo^{5+} (3d) CT transition is predominant at low Ni contents. It is consequently concluded that the presence of TEG influences the structure and/or the location of surface molybdenyl species forcing them to interact more strongly with Ni species.

A possible interpretation, based on previous data concerning multiple impregnation of oxides on oxide [23], is the following. Metal ionic species, when are interacting at the surface of metal oxide

surfaces such as alumina, behave in relation to their acido-basic nature. Both Ni^{2+} and MoO^{4+} (molybdenyl) ions are Lewis acidic in nature and will compete with each other for the interaction on the most basic sites of the alumina surface. However, to preserve neutrality, their charge has to be compensated by (oxide or hydroxide) anions that will also adsorb on the support surface. The ionic pairs will interact with the most exposed acido-base pairs of the support surface.

Spectral data indicate (e.g. adsorption of pyridine on molybdena-based solids and Ni^{2+}-containing solids) that molybdenyl species with their paired anions are more ionic than Ni^{2+}ions and their corresponding anions. Thus molybdenyl species will interact with the strongest acido-basic sites of the alumina surface forcing the Ni^{2+} ions to shift over to weaker acido-basic surface sites. This is the reason why the d-d Ni^{2+} transitions for NiO/Al_2O_3 are very different from those observed in $NiMo/Al_2O_3$ species.

However, TEG (as any alcohol) adsorbs on alumina over Lewis acid sites through its oxygen lone pair [24]. Thus, TEG is able to shift surface molybdenyl species from the strongest acido-basic sites of alumina, to weaker ones, where their interaction with Ni can become more likely. It seems quite reasonable to suppose that the strongest acido-basic sites of the alumina surface are on the surface defects (edges and corners, or terraces, over the surface of the microcrystals). Thus TEG will shift the molybdenyl species from the surface defecting sites forcing them to migrate to plane crystal faces, where interaction with alumina is weaker and interaction with nickel may be easier. The location of both Mo and Ni species on the plane faces favors their interaction, that is, the formation of Ni-Mo species that will contribute to the formation of a well promoted Ni-Mo-S phase; the lower interaction with the alumina surface in plane crystal faces can be lowered even more by the interaction of TEG with the alumina surface; this will favor a better sulfidation of the Mo species. This explanation is consistent with the observed formation of heteropolycompounds in the case of $CoMoP/Al_2O_3$ catalysts in which preparation was used a glycol compound [5,6,9]

4. Conclusions

The interaction of triethylene glycol (TEG) with alumina and its role in preparing improved $NiMo/Al_2O_3$ hydrodesulfurization catalysts has been investigated by spectroscopic methods. From the results of the study it can be concluded that the catalyst prepared with TEG is more active in the HDS of 4,6-dimethyldibenzothiophene than a similar catalyst prepared without the additive and following the conventional method of impregnation, drying, calcination, and sulfidation. The higher activity of the catalyst prepared with TEG (2.5 times more active) can be explained because:

- TEG adsorbs mainly on the corners, edges, and other defects of alumina microcrystals where the strongest Lewis sites and the higher νOH frequency hydroxyl groups are mainly located.
- TEG and their decomposition products, formed upon heating (mainly acetates) occupy the strongly interacting edge and corner sites of the alumina crystals, forcing the Mo and Ni

species to migrate mainly to the plane faces of alumina. This weakens the metal-support interaction allowing a better sulfidation and, at the same time, favors the Ni-Mo interaction and the formation of the promoted NiMoS phase.

- TEG does not modify significantly the d-d transitions of Ni^{2+}, while shifts and broadens the charge transfer transition region, where the O^{2-} (2p) $\rightarrow$ Mo^{5+} (3d) CT transition is predominant. Therefore TEG does not modify the electronic structure of Ni but it does so with Mo. This suggests that TEG interacts preferable with edges and corners of the alumina support particles, where Mo is preferable deposited. The addition of TEG does not modify the anchoring site of the Ni oxide precursor.
- The IR study of CO adsorbed on the reduced/sulfided NiMo catalysts confirm that the amount of sulfide phase increases in the samples prepared with TEG, indicating that TEG induces a better sulfidation of the oxide precursors, thus favoring the formation of the more active type II NiMoS sites.

5. **Acknowledgments**

The authors acknowledge funding from Italy (MAE)-Mexico (CONACyT) exchange program and to DGAPA-UNAM through the PAPIIT IN-114112 program. To I. Puente-Lee for the HRTEM work.

Figure Captions

Figure 1. FTIR spectra for γ-Al_2O_3 (---) and γ-Al_2O_3-TEG (-), after outgassing at several temperatures.

Figure 2.FT-IR spectra of liquid TEG+KBr mixture (---) as reference and subtraction spectra of γ-Al_2O_3-TEG(-) sample after outgassing at several temperatures. ESTE PIE DE FIGURA NO DESCRIBE BIEN LO QUE SE MUESTRA QUIERO REHACER LA FIGURA

Figure 3. Subtraction FTIR spectra of pyridine species on Al_2O_3 (full lines) and Al_2O_3-TEG (broken lines) both pre-activated by outgassing at 473 K. The spectra are recorded in contact with the pyridine vapor (top), after outgassing at r.t. (middle) and at 373 (bottom).

Figure 4. FTIR spectra for the NiMoT catalyst upon outgassing at increasing temperature and Al_2O_3 support as reference.

Figure 5. FTIR subtraction spectra of the NiMoT catalyst precursor upon outgassing at increasing temperature. The spectrum recorded after outgassing at 773 K is subtracted from the others.

Figure 6. UV-vis DR spectra at room temperature.

Fig. 7 IR spectra of CO adsorbed (1 Torr equilibrium) at low temperature over NiMo (full line) and NiMoT (dash line) catalysts.

References

[1] Patent EP 0601722 B1 (1994) Sumitomo Metal.

[2] Patent WO 96/41848A1, 1996.

[3] Patent EP 1418002 A2, 2004

[4] N. Iwamoto, A. Kagami, J. Lino, J. Jap. Petrol. Inst. 48(4) (2005) 237-242.

[5] D. Nicosia, R. Prins, J. Catal. 229 (2005) 424–438.

[6] D. Nicosia, R. Prins, J. Catal. 231 (2005) 259–268.

[7] V. Costa, K. Marchand, M. Digne, C. Geantet, Catal. Today 130 (2008) 69–74.

[8] T. Son Nguyen, S. Loridant, L. Chantal, T. Cholley, C. Geantet, Appl. Catal. B: Environmental 107 (2011) 59– 67.

[9] V. Costa, B. Guichard, M. Digne, C. Legens, P. Lecour, K. Marchand, P. Raybaud, E. Krebs, C. Geantet, Catal. Sci. & Tech. 3 (2013) 140-151.

[10] J. Escobar, M.C. Barrera, J.A. Toledo, M.A. Cortés-Jácome, C. Angeles-Chávez, S. Nuñez, V. Santes, E. Gómez, L. Díaz, E. Romero, J.G. Pacheco, Appl. Catal. B: Environ. 88 (2009) 564–575.

[11] H. Yin, T. Zhou, Y. liu, Y. Chai, C. Liu, J Fuel Chem Technol 2011 39(2), 109−114.

[12] H. Topsøe, Appl. Catal. A: Gen. 322 (2007) 3-8.

[13] O. B. Zubkova, A. N. Shabadash, J. Appl. Spectr. 14 (1971) 639-643.

[14] G. Busca, Catal. Today in press http://dx.doi.org/10.1016/j.cattod.2013.08.003

[15] M. A. Peluso, E. Pronsato, J. E. Sambeth, H. J. Thomas and G. Busca, Appl. Catal. B: Environmental, 78 (2008) 73-79.

[16] M. I. Zaki, M. A. Hasan, F. A. Al-Sagheer, L. Pasupulety, Colloids and surfaces A: Physicochemical and Engineering aspects, 190 (2001) 261-274.

[17] G. Busca and J.C. Lavalley, Spectr. Acta 42 A (1986) 443-445.

[18] G. Busca, J. Raman Spec. 33 (2002) 348-358.

[19] J. Ramirez, L. Cedeño, G. Busca, J. Catal. 184 (1999) 59–67.

[20] M.A. Larrubia, G. Busca, Materials Chemistry and Physics 72 (2001) 337–346.

[21] D. Nikolova, R. Edreva-Kardjieva, M. Glurginca, A. Meghea, J. Vakros, G.A. Voyiatzis, C. Kordulis, J. Vib. Spectrosc. 44 (2007) 343-350.

[22] A. Travert, C. Dujardin, F. Mauge´, E. Veilly, S. Cristol, J.-F. Paul, E. Payen, J. Phys. Chem. B 110 (2006) 1261-1270.

[23] G. Ramis, G. Busca and F. Bregani, Catal. Lett. 18 (1993) 299-303.

[24] G. Busca, P.F. Rossi, V. Lorenzelli, M. Benaissa, J. Travert, J.C. Lavalley, J. Phys. Chem. 89 (1985) 5433-5439.

[25] G. Busca, P.F. Rossi, V. Lorenzelli, M. Benaissa, J. Travert and J.C. Lavalley, J. Phys. Chem. 89 (1985) 5433-5439.

Table 1. Catalytic activity in the Hydrodesulfurization of 4,6-Dimethyldibenzothiophene (T=593 K and 1200 psig), and dispersion for the prepared catalysts.

Catalyst	k ($L/h\text{-}g_{CAT}$)	k_{DDS}* ($L/h\text{-}g_{CAT}$)	k_{HYD}* ($L/h\text{-}g_{CAT}$)	k_{HYD}/k_{DDS} ($L/h\text{-}g_{CAT}$)	$TOFx10^4$ (h^{-1})	Dispersion
NiMo	0.088	0.016	0.072	4.5	1.9	0.31
NiMoT	0.232	0.026	0.205	7.88	4.6	0.35

*Calculated for $X_{4,6\text{-DMDBT}}$ =30%

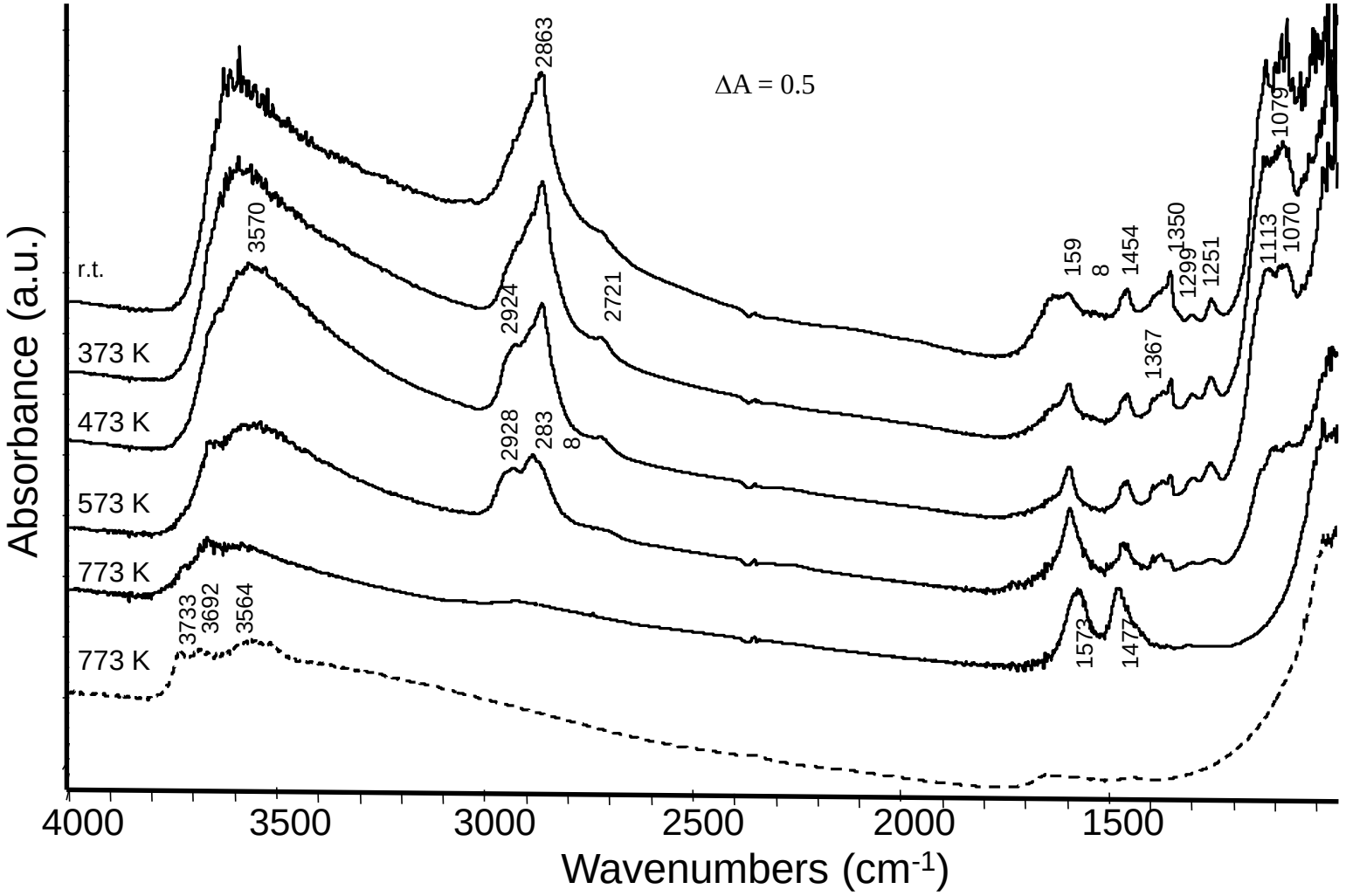
ΔA = 0.5
Absorbance (a.u.)
Wavenumbers (cm-1)
4000
3500
3000
2500
2000
1500
r.t.
373 K
473 K
573 K
773 K
773 K
3570
2863
2924
2721
2928
2838
3733
3692
3564
1598
1454
1350
1299
1251
1113
1079
1070
1367
1572
1477

Figure 1

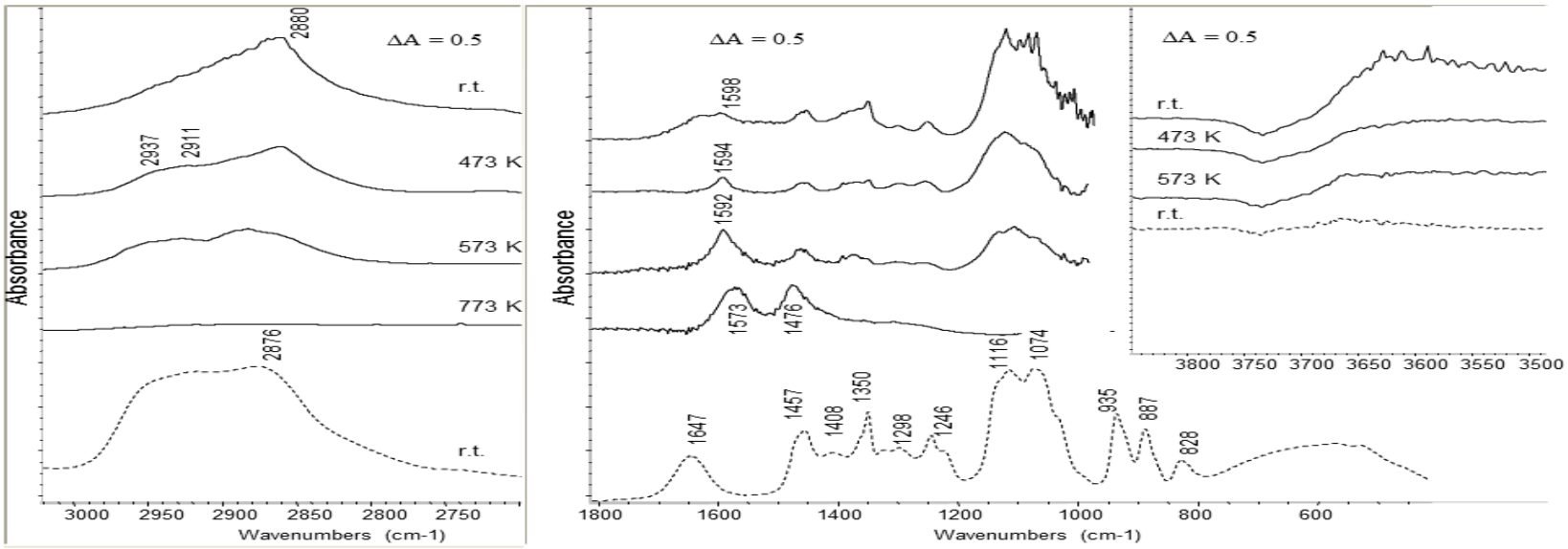
ΔA = 0.5
r.t.
473 K
573 K
773 K
r.t.
2880
2937
2911
2876
Absorbance
3000
2950
2900
2850
2800
2750
Wavenumbers (cm-1)
ΔA = 0.5
1598
1594
1592
1573
1476
1647
1457
1408
1350
1298
1246
1116
1074
935
887
828
1800
1600
1400
1200
1000
800
600
Wavenumbers (cm-1)
ΔA = 0.5
r.t.
473 K
573 K
r.t.
3800
3750
3700
3650
3600
3550
3500

Figure 2

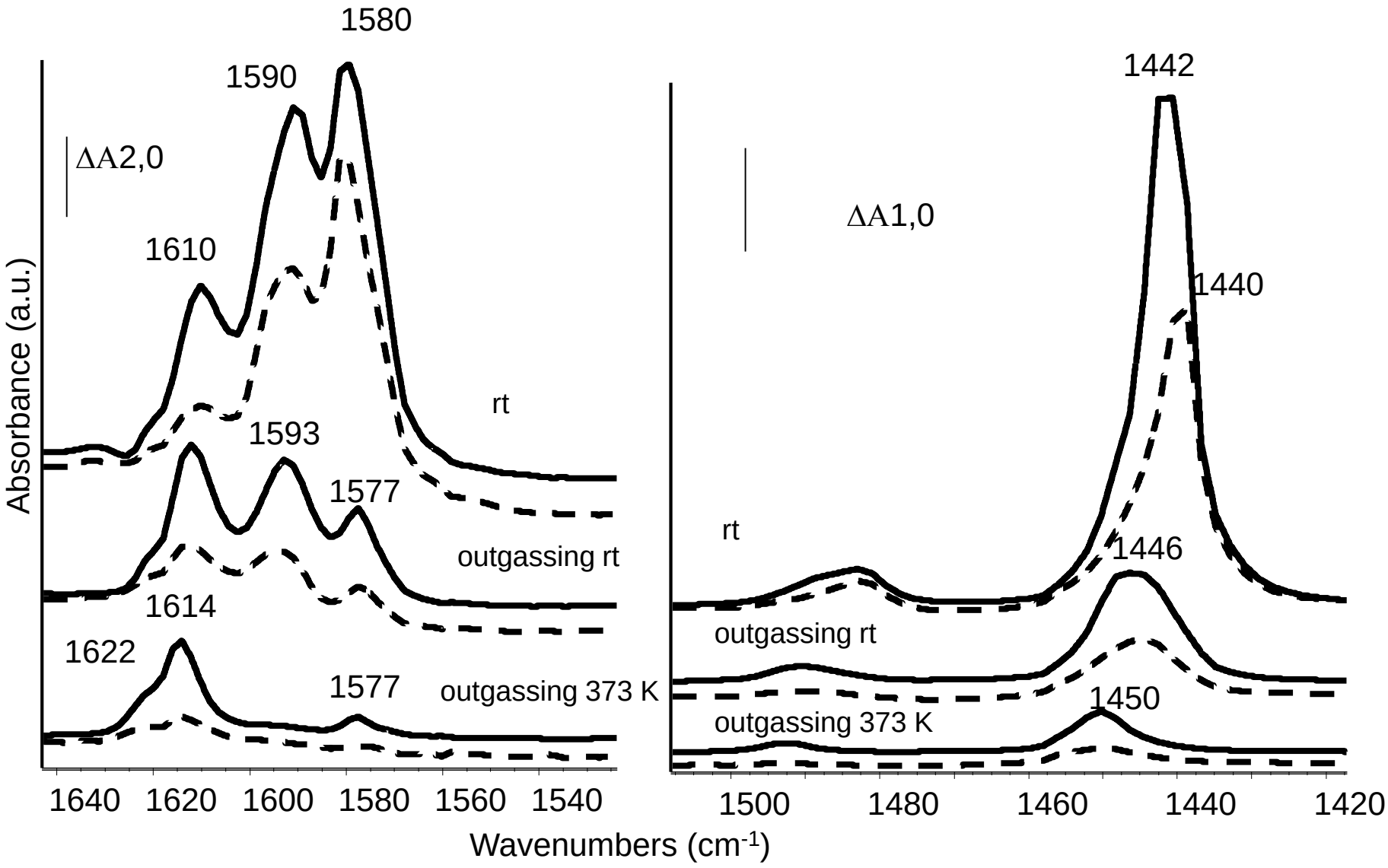
1580
1590
ΔA2,0
1610
rt
1593
1577
outgassing rt
1614
1622
1577
outgassing 373 K
Absorbance (a.u.)
1640
1620
1600
1580
1560
1540
1442
ΔA1,0
1440
rt
1446
outgassing rt
1450
outgassing 373 K
1500
1480
1460
1440
1420
Wavenumbers (cm-1)

Figure 3

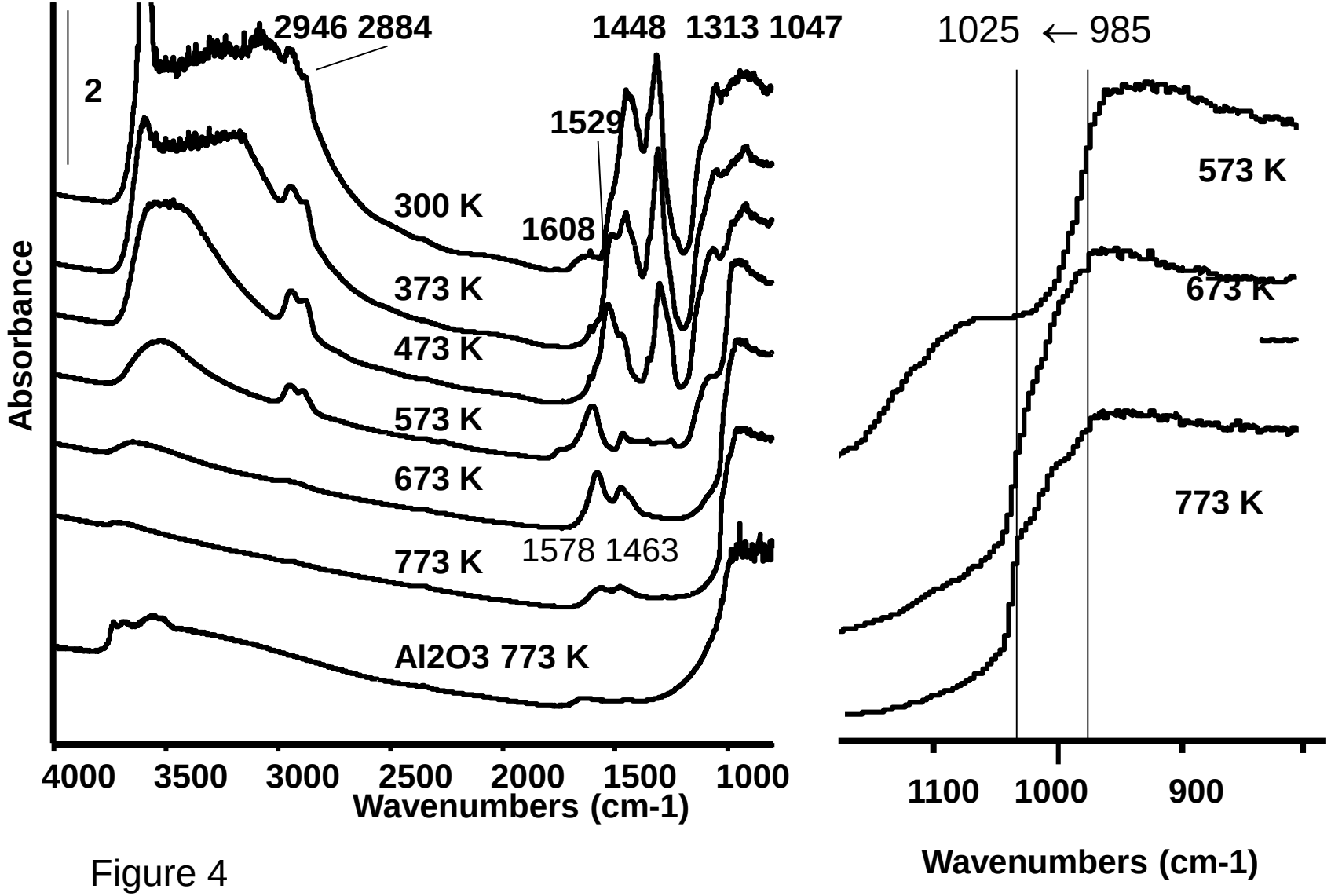
2946 2884
1448 1313 1047
1025 ← 985
2
1529
300 K
1608
373 K
473 K
573 K
673 K
773 K
1578 1463
Al2O3 773 K
Absorbance
4000 3500 3000 2500 2000 1500 1000
Wavenumbers (cm-1)
573 K
673 K
773 K
1100 1000 900
Wavenumbers (cm-1)

Figure 4

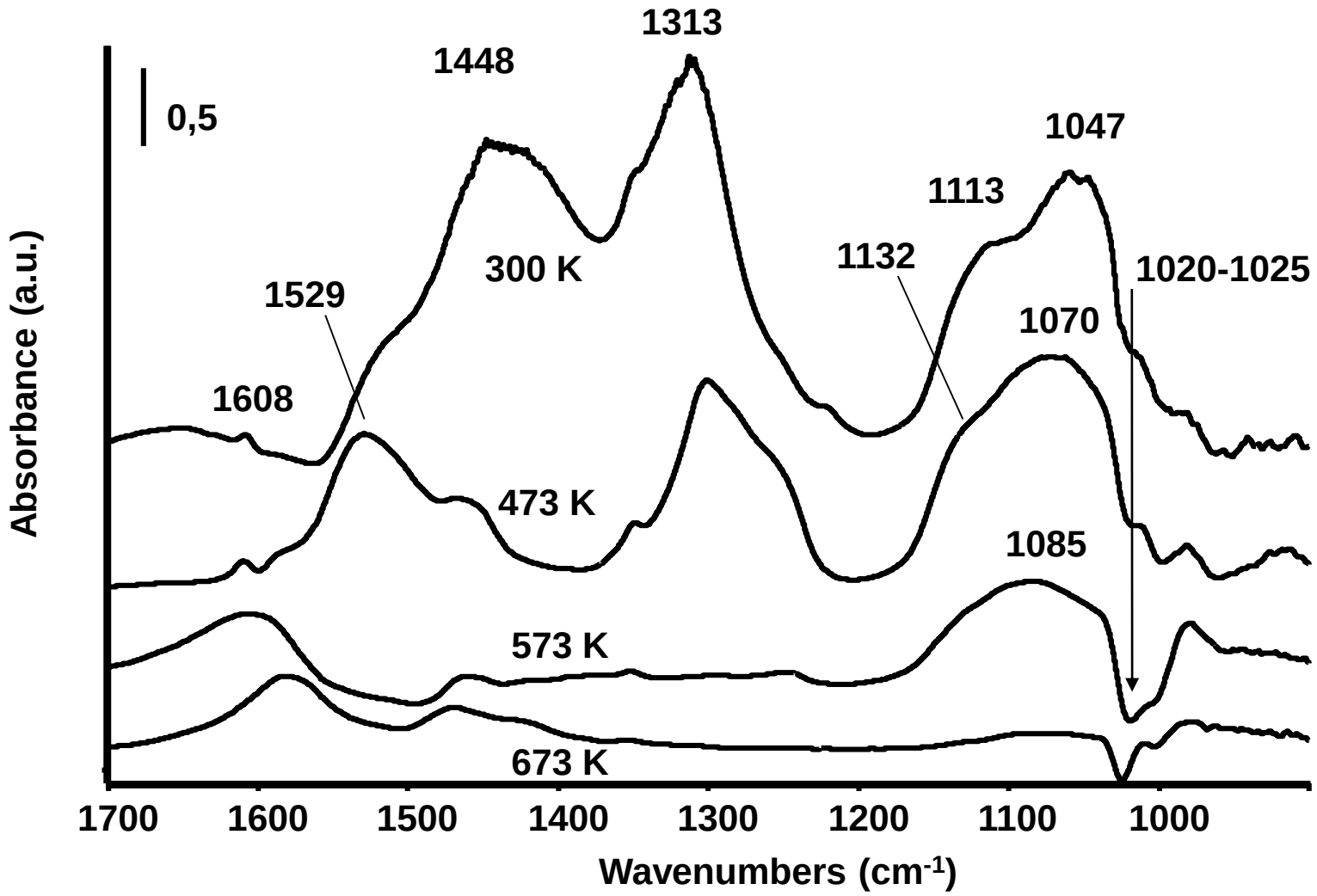
1313
1448
0,5
1047
1113
1132
1020-1025
300 K
1529
1070
1608
473 K
1085
573 K
673 K
Absorbance (a.u.)
1700
1600
1500
1400
1300
1200
1100
1000
Wavenumbers (cm-1)

Figure 5

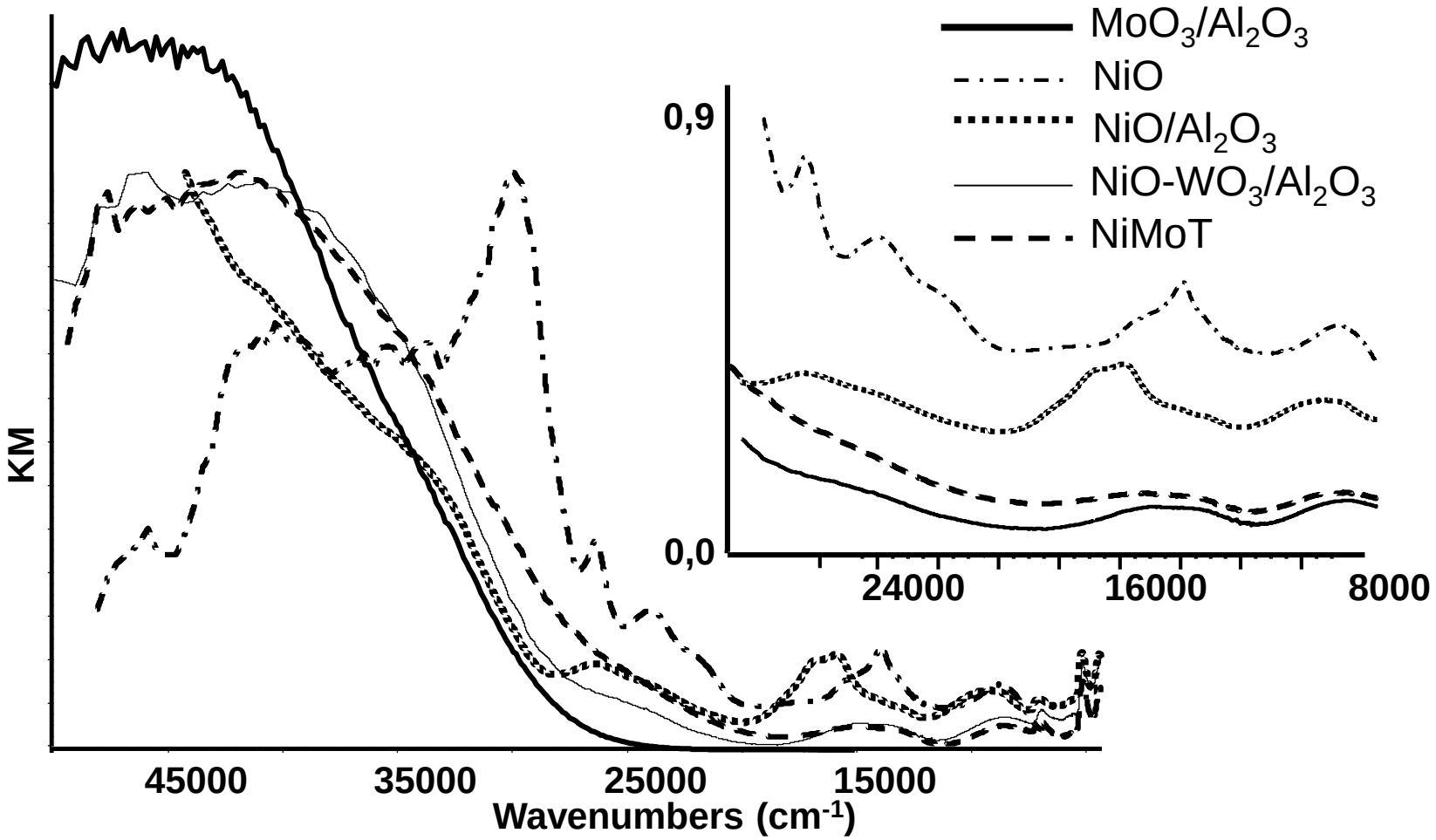
MoO3/Al2O3
NiO
NiO/Al2O3
NiO-WO3/Al2O3
NiMoT
KM
0,9
0,0
24000
16000
8000
45000
35000
25000
15000
Wavenumbers (cm-1)

Figure 6

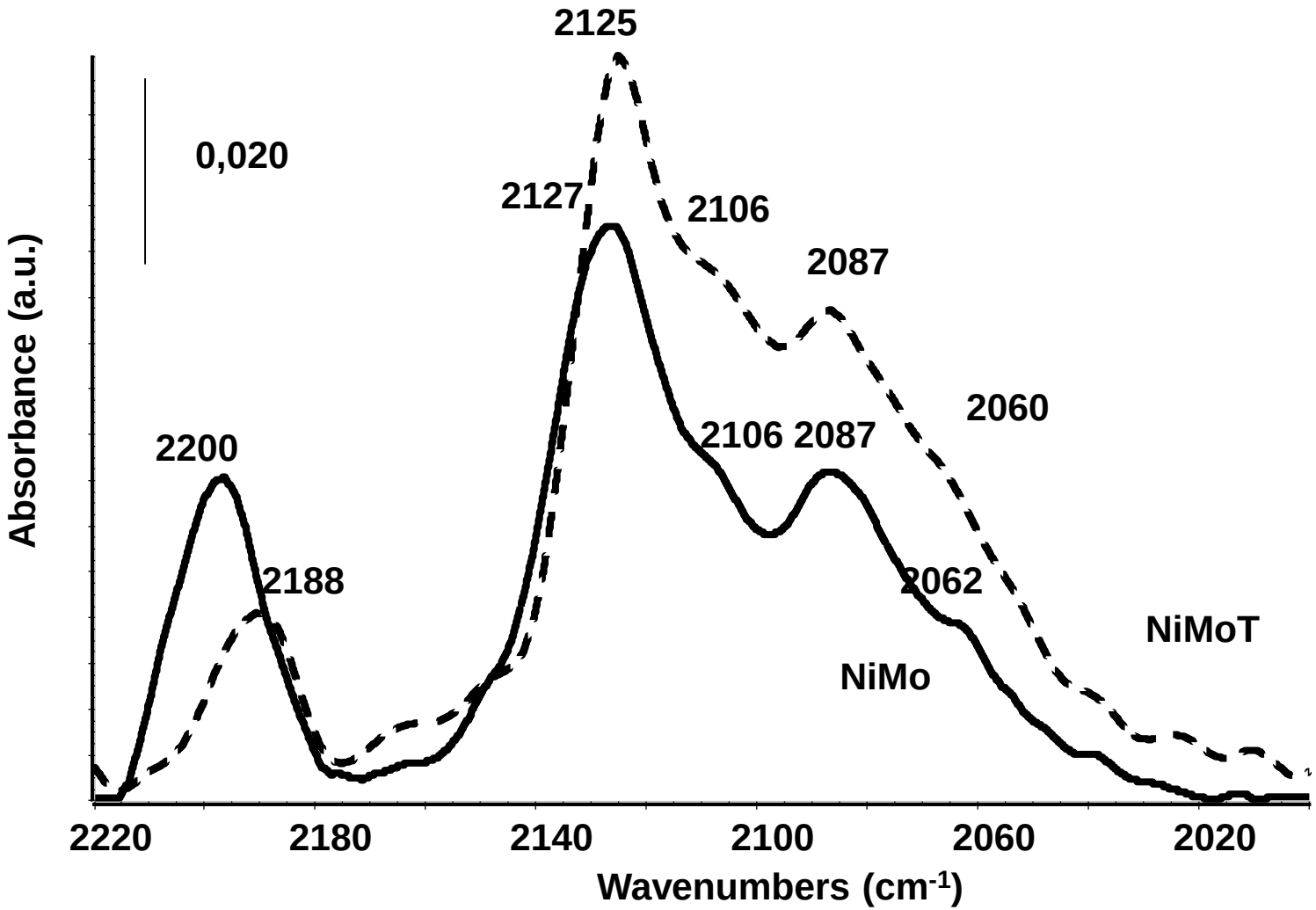
2125
0,020
2127
2106
2087
2060
2200
2106 2087
2188
2062
NiMoT
NiMo
Absorbance (a.u.)
2220
2180
2140
2100
2060
2020
Wavenumbers (cm-1)

Figure 7